Proceedings of the Sixth International Conference on
Railway Technology: Research, Development and Maintenance
Edited by: J. Pombo
Civil-Comp Conferences, Volume 7, Paper 4.11
Civil-Comp Press, Edinburgh, United Kingdom, 2024
ISSN: 2753-3239, doi: 10.4203/ccc.7.4.11

Convergence Study for the Simulation of Stitched Railway Catenary Dynamics and Design Verification of a High-Speed System for Sweden

B. Schick, W. Z. Liu and S. Stichel

**Department of Engineering Mechanics,
KTH Royal Institute of Technology
Stockholm, Sweden**

Abstract

This paper describes the results of a parametric convergence study on dynamic pantograph-catenary interaction simulations performed with the simulation tool CaPaSIM 3D. The convergence study has been part of validating the latest version of CaPaSIM 3D following EN 50318:2018. The effects of adjusting parameters in the simulation setup on the results are shown and how they can be chosen to obtain results within the required ranges for all relevant metrics for verifying a new system design. However, the convergence study also shows that some of the specified result ranges for the simulation of stitched catenary systems conflict with convergence trends for the performed simulations. These conflicts are described and discussed. In addition, simulation results verifying the dynamic interaction characteristics of the design proposal for a new Swedish overhead catenary system for high speeds are shown. These results show that the system design is expected to fulfil the requirements of the TSI Energy. General conclusions regarding the implications of studying overlap sections and multiple pantograph operation are drawn from this example.

Keywords: validation, railway, pantograph, power supply, finite element analysis, dynamic interaction.

1 Introduction

The functional interaction between the pantograph and the overhead catenary line (OCL) is crucial for the safe and reliable operation of electric railways [1]. This is illustrated by the fact that failures in the interaction can lead to damages that are among the most severe and time-consuming to repair on the railway infrastructure. Simulation tools have been developed during the past decades and have become highly reliable and valuable for creating and verifying OCL system designs [2]. This includes the specifications for new system types [3] or to obtain design solutions for specific track sections [4].

Typically using Finite Elements FE as a computational method, the dynamic simulations are highly sensitive to the choice of setup parameters such as mesh layout, element choice and boundary conditions. Therefore, a continuous effort has been made to find reliable levels of computational resolution [5], [6]. Another crucial aspect is the structural damping and how it is considered in the simulations. There are recommendations given in the standards, but they are mainly based on conclusions from literature studies and common practices for matching measurement results [7]. Recent measurements explicitly focus on the structural damping characteristics of the OCL components; however, they show that further development should be carried out to consider the findings in dynamic simulations [8], [9]. In addition to that, other limitations remain, for example, in the validated frequency ranges of the study.

The study presented in this paper performs the convergence study on the setup parameters for the latest version of CaPaSIM 3D to ensure that the results align with the literature. In addition, the effect of boundary conditions, the simulation's initialisation procedure, and structural damping coefficients are studied. In a final step, these results are applied to another simulation series performed for the system design verification of Sweden's new high-speed catenary system according to the TSI Energy [10].

2 Methods

CaPaSIM 3D is a simulation tool for pantograph-catenary interaction developed in cooperation between KTH Royal Institute of Technology and Trafikverket. It uses the commercial software ANSYS Mechanical APDL to perform the Finite Element (FE) simulations that are the central part of the tool. In the latest version, the tool automatically processes the input geometry, creating the input scripts for the dynamic FE solver based on various parameter choices. A FE representation of the catenary structure, represented in the original three-dimensional straight track geometry, is used for static and dynamic simulations. This means that the choice of element types and the mesh resolution can be adjusted to ensure the required result quality. The effects of these adjustments are studied in this paper. The accurate dynamic behaviour is also ensured by considering dropper slacking and modelling the steady arm explicitly as a moving body in the 3D structure, as shown in Figure 1. The pantograph model follows the conventional lumped setup with up to three levels of mass, spring, and damper elements. Depending on the parameter set used for the pantograph, bump-stops and frictional effects can also be considered. Alternatively, the top mass level can be modelled by two separately suspended lumped masses or bodies.

Before dynamic simulation, the catenary geometry is verified and adjusted in a series of iterative static simulations. In these iterations, the alignment and tension of the stitch wires and the steady arm fixture points are adjusted to ensure the correct alignment of the contact wire in the vertical and lateral directions.

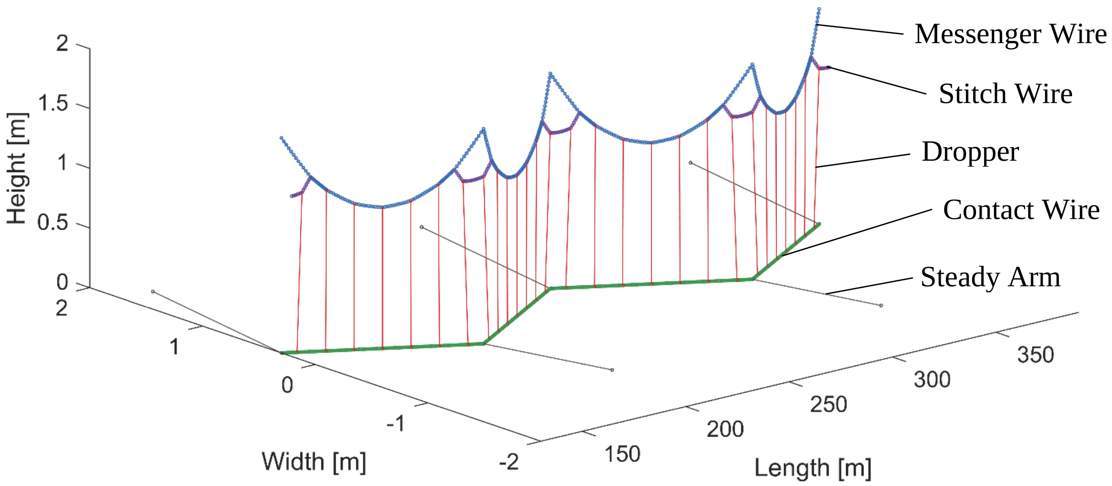

Figure 1: 3D view of catenary geometry with alignment of finite elements.

The contact between the pantograph and the contact wire is modelled with the penalty method, using a contact stiffness k_c of 50 N/mm to calculate the contact force F_c based on the intersection depth δ_c between the contact wire and collector elements.

$$F_c = \begin{cases} k_c \delta_c \text{ if } \delta_c > 0 \\ 0 \quad \text{if } \delta_c \leq 0 \end{cases} \tag{1}$$

For time integration, the performance of the Newmark and the generalised HHT-α method [11] were compared in the dynamic simulations. The variation of the 2nd-order numerical integration coefficients is considered for the numerical convergence. Structural damping is applied following the system specifications in the standard. Another studied variation is the applied boundary conditions for model initialisation. The first approach locks the ends of the contact wire in the vertical direction and lets the pantograph start from the nominal contact wire height. In contrast, the second approach does not lock the contact wire ends vertically and instead initialises all pantographs in a statically balanced uplift position before starting the transient dynamic simulation.

The simulation results are evaluated by calculating the dynamic contact force F_d between the pantograph and catenary, performing aerodynamic inertial correction equivalent to measurement processing described in EN 50317 [12]. All the evaluated force and displacement signals are low pass filtered using a Butterworth filter of order 10 and a cut-off frequency of 20 Hz. The contact force standard deviation in the specific frequency ranges of 0-5 and 5-20 Hz are evaluated using the Fast Fourier Transform (FFT) of the unfiltered force signal.

3 Results

As a first validation step, a section of 18 identical ideal spans of the reference model AC stitched specified in EN 50318 [7] is modelled. The four spans at each end are excluded from the evaluation to obtain the specified analysis section of 10 spans. The convergence study is performed after ensuring the correct static representation of the catenary structure. Based on that, a parameter setup is presented, producing simulation results within the acceptable range specified in the standard [7].

3.1 Static comparison to the reference model

An overview of the modelled catenary structure's static characteristics and its comparison to the nominal values is shown in Figure 2. This level of agreement is achieved by using the iterative correction loop and is independent of the parameter choices described in the following chapter. Therefore, it is mainly the dynamic behaviour that is of interest for further studies.

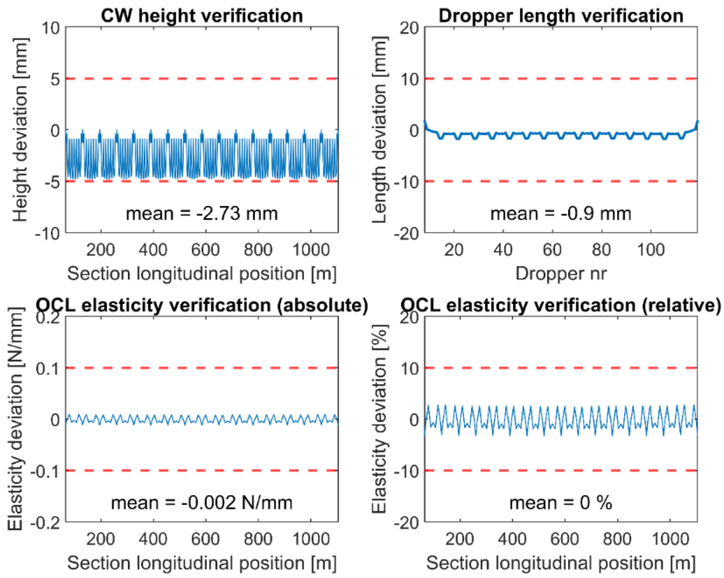

Figure 2: Comparison of static catenary model characteristics to reference values.

3.2 Convergence study

The convergence study considers the effects of boundary conditions, changed element types, increased mesh resolution, reduced time step, and change in integration coefficients. The results presented below are limited to the case with a higher speed v of 320 km/h, as they are more sensitive to the changes in the setup.

Before changing the mesh setup, the effect of changing the element types is studied, as shown in Figure 3. An initial study using the original boundary conditions with vertically fixed wire ends shows that the dynamic variations of the contact forces for the trailing pantograph decrease when the link elements in messenger and stitch wire are replaced by Euler-Bernoulli beams. However, the variations increase again when the Euler-Bernoulli beams used in the contact wire are replaced by Timoshenko beams. The increase is even larger when the same is done with the beams of messenger and stitch wires.

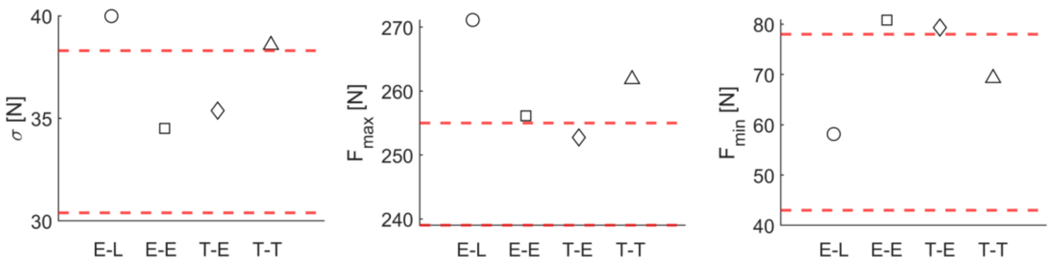

Figure 3: Effect of the used element types on the simulation results for the trailing pantograph at v = 320 km/h. The first letter indicates the contact wire elements, the second messenger and stitch wire [E – Euler-Bernoulli beam, L – Link, T – Timoshenko beam].

For the study of the influence of element length and time step, a maximal element length is set, and the mesh resolution of each individual part in the structure is doubled until no element remains above the length limit. The same limit is applied to all wires in the structure. When the boundary conditions and initialisation procedure described in section 3 are changed from the vertically locked to the free and initially balanced contact setup, a drastic reduction of the contact force variations is observed. The convergence patterns are, however, similar and especially pronounced in the contact force standard deviation σ. Figure 4shows the convergence pattern for the original and updated boundary conditions, respectively. The common pattern is that the results stabilise at a maximal element length of 0.5 m and a time step of 1 ms. Some of the results remain, however, consistently outside the ranges given in the standard.

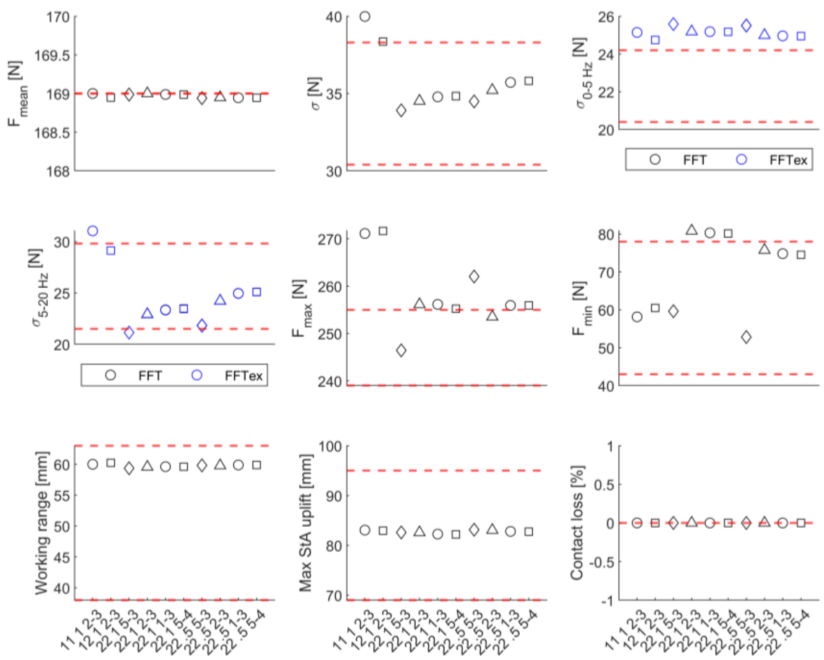

Figure 4: Effect of the decreasing element length and time step length before the update of the boundary conditions for the trailing pantograph at v = 320 km/h. The first two data points in each box use links for messenger and stitch wire.

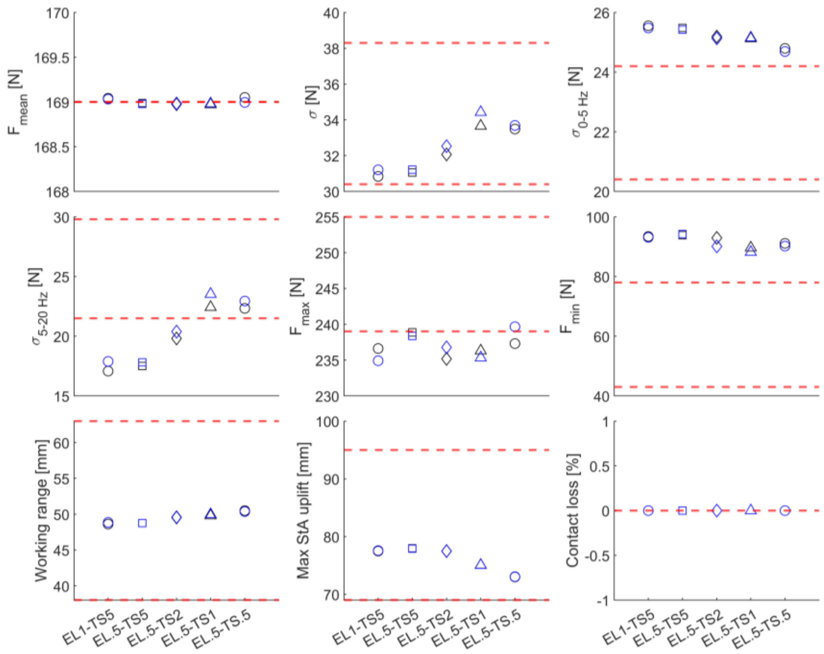

Figure 5: Effect of decreasing element length and time step length after the update of the boundary conditions for the trailing pantograph at v = 320 km/h. The blue data points are obtained using Timoshenko beams for the contact wire.

The comparison of Euler-Bernoulli and Timoshenko beams for the contact wire is repeated with the updated boundary conditions. As shown in Figure 5, the differences in the results are small to non-existent. Therefore, the substantially higher computation cost of using the higher-order Timoshenko beams cannot be motivated. The comparison of the integration methods shows that the generalised HHT-α method is slightly more computationally efficient than the Newmark method for the given problem. The results from both methods show, however, a high sensitivity to the choice of integration parameters. They affect the contact force dynamics, especially in the higher frequency range towards 20 Hz, to a greater extent than the changed beam type in the contact wire or the final changes to element length and time step. However, as they should only be increased to ensure a stable numerical solution, the approach chosen for this study is to calculate the coefficients from a numerical damping coefficient $\gamma = 0.05$. The final setup and its results are described in the next section.

3.3 Dynamic comparison to the reference model

A setup with Euler-Bernoulli beams for all wires, a maximum element length of 0.5 m, free contact wire ends, and the statically stable initialisation are used for the dynamic validation. Simulations are performed using the generalised HHT-α method with a time step of 1 ms and 2nd-order transient integration coefficients calculated from a numerical damping coefficient $\gamma = 0.05$. Figure 6 and Figure 7 show that the results are within the ranges of 5 comparison metrics for all evaluated cases. These are the mean contact force F_{mean}, the standard deviation of the contact force σ, the pantograph vertical working range, the maximum uplift of the contact wire at the steady arm, and the contact loss ratio.

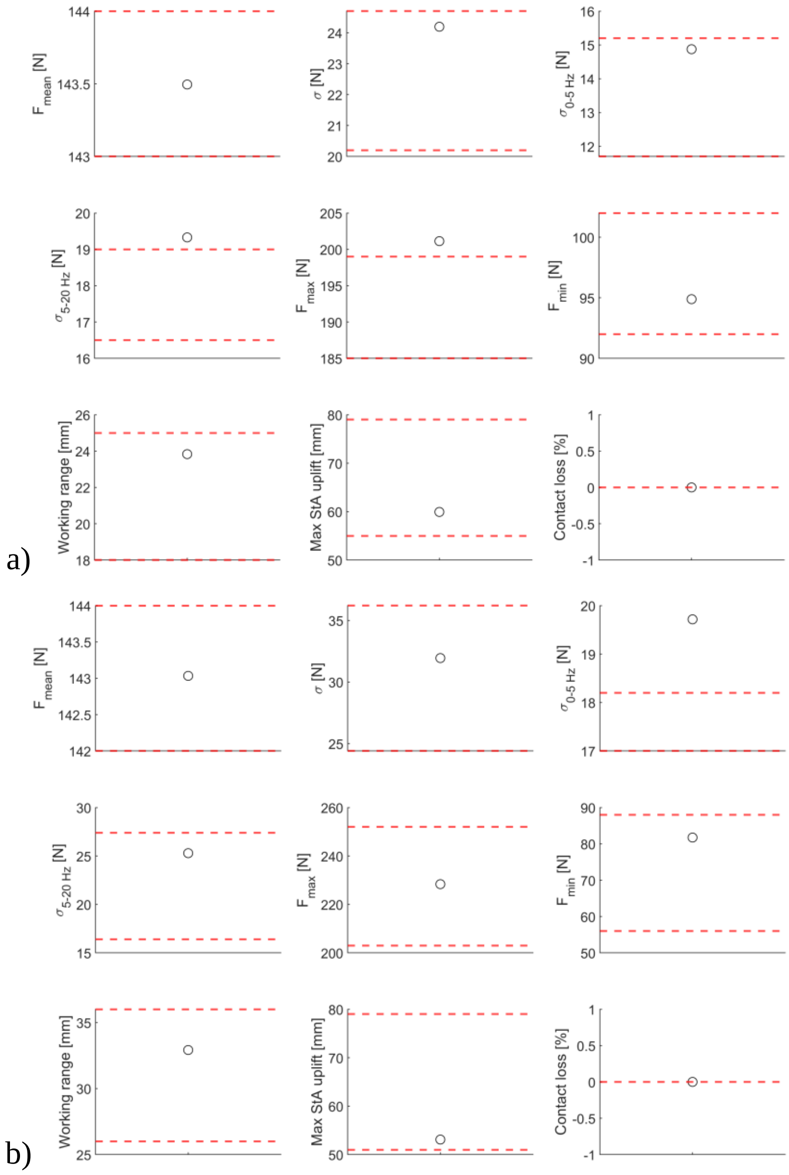

Figure 6: Comparison of the dynamic results to the acceptable ranges for the leading pantograph (a) and the trailing pantograph (b) at v = 275 km/h.

Deviations from the ranges given by the standard occur for the trailing pantographs in the contact force standard deviation in the specific frequency range of 0-5 Hz. Figures 5b) and 6b) show that $\sigma_{0\text{-}5}$ considerably exceeds the acceptable range for these cases. At 275 km/h, $\sigma_{5\text{-}20}$ is above the acceptable range for the leading pantograph instead. However, these deviations do not affect the reliability of the simulation tool for verifying the new system design according to the TSI norm because σ is there to be evaluated for the entire frequency range of 0-20 Hz. The results for σ in the whole frequency range are accurate.

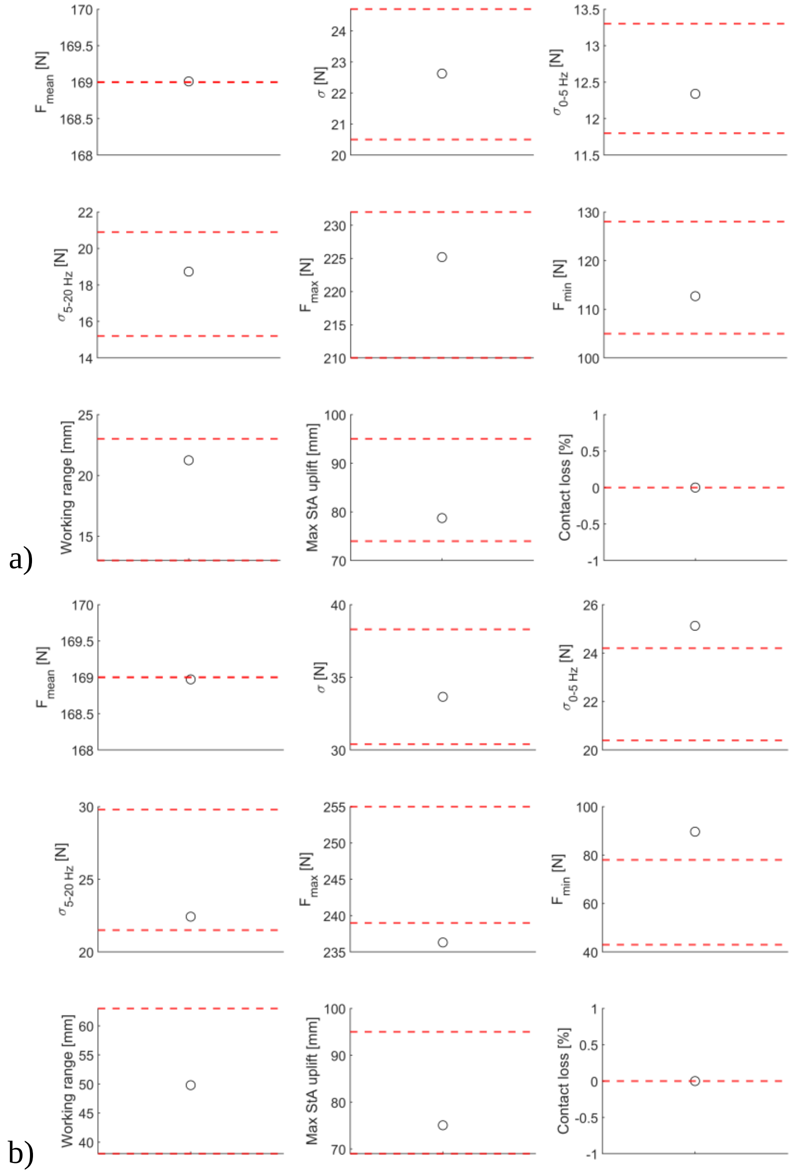

Figure 7: Comparison of the dynamic results to the acceptable ranges for the leading pantograph (a) and the trailing pantograph (b) at v = 320 km/h.

In addition, the maximum actual contact force F_{max} slightly exceeds the acceptable range for the leading pantograph at 275 km/h. Such an overestimate would make the simulation results somewhat conservative. In contrast, the dynamic variations on the trailing pantograph at 320 km/h are much lower in terms of F_{max} and F_{min} than the values given by the standard. Such a pattern is more problematic, as it can provide too optimistic expectations of dynamic interaction behaviour. The convergence patterns, however, indicate that the result is numerically correct, given the system parameters. This makes it highly relevant to compare these results to a broader set of validation data based on measurements. This comparison will be added in a later stage of the study.

3.4 Verification of the proposed system design

Simulations are performed for the verification of the proposed system design, which is a Swedish adaptation of the stitched AC system in [7]. The speed range is 220 to 360 km/h, which exceeds the design speed of 320 km/h, to find the margins in the expected interaction characteristics. For the pantograph models, validated parameter sets for the DSA 200.56 and DSA 380D type pantographs were provided by the manufacturer. The effect of structural damping reduction and the implications of modelling overlap sections on multiple operation are studied during this simulation process.

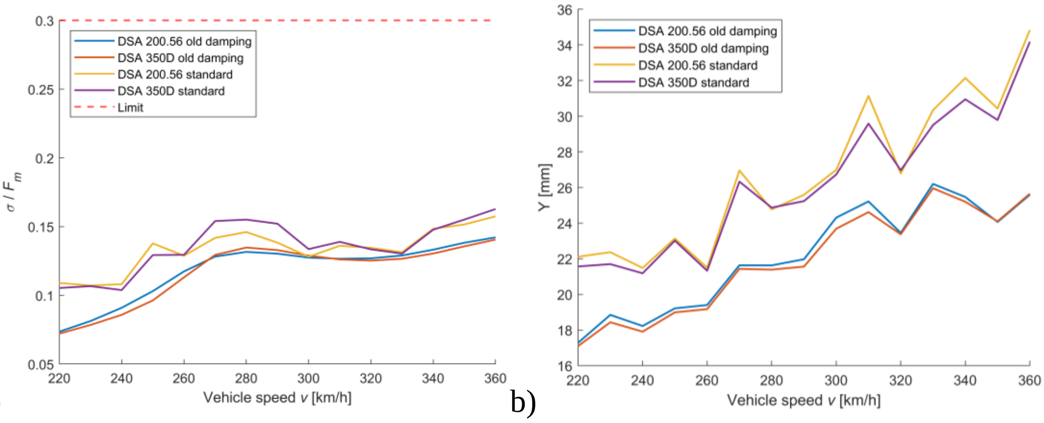

a) b)

Figure 8: Comparison of standard deviation ratio (a) and pantograph vertical working range (b) for two different pantographs in single operation.

The results in Figure 8 show that reducing the structural damping coefficient from 2 % to the 0.1 % recommended in the standard does not drastically change the standard deviation σ, which remains far below 30 % of the mean contact force F_m. However, the effects on the working range are more noticeable, and local maxima due to resonance effects become more pronounced. Therefore, the reduction of structural damping can be expected to have more substantial implications for the simulation of operation with two or more pantographs and the consideration of critical sections.

The implications of operation with two pantographs are studied by comparing the dynamic results of running on an ideal section to results from two or three sections with section overlaps. For the latter cases, the studied interaction distance was cut by half a section at each end to obtain a representative proportion between the overlap and ideal spans. The DSA 380D pantograph model is used for all simulations. The results of the overall dynamic variations in the contact force, most prominently the standard deviation σ, are almost identical for the two studied cases, as shown in Figure 9. The most noticeable differences are found in the maximal uplift at the steady arm Δy_{StA}, the maximal uplift at the span mid Δy_{mid} and the vertical working range Δy_{panto}. Figure 10 and Figure 11 show that all values are considerably higher when the overlap section is considered.

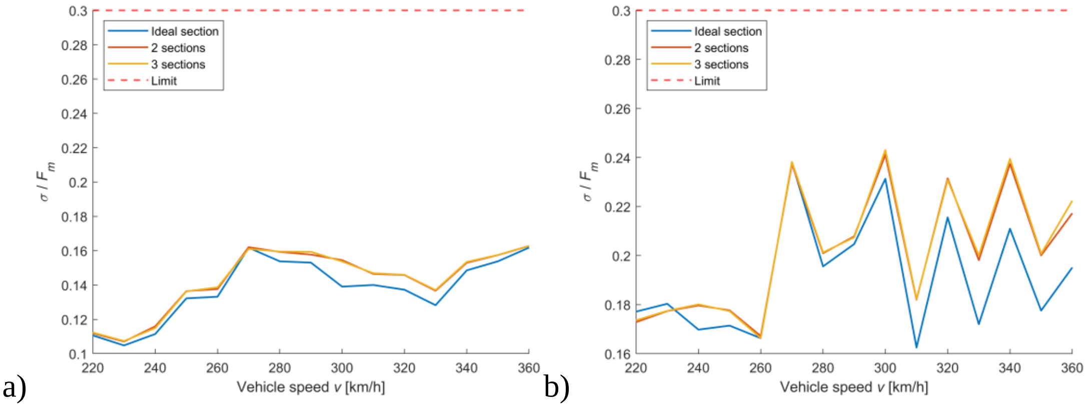

Figure 9: The ratio of σ/F_m for the leading (a) and the trailing (b) pantograph in multiple operation at a distance of 165 m.

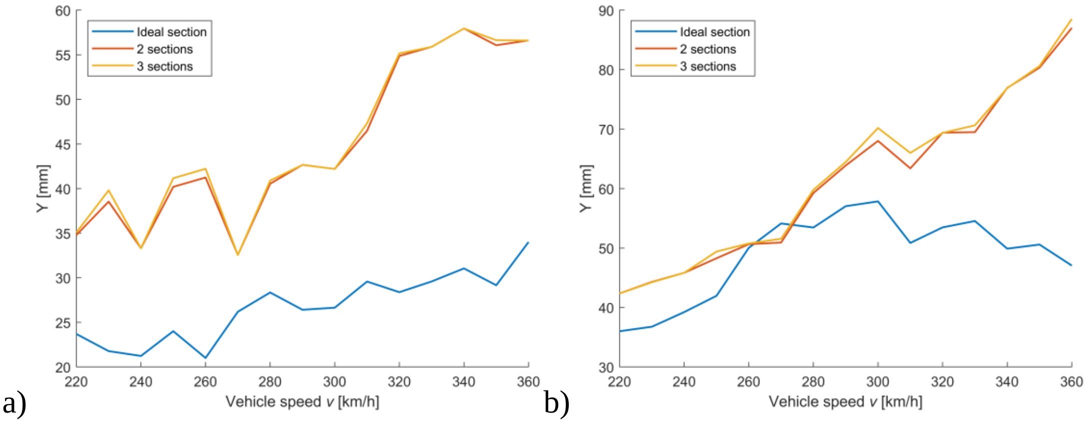

Figure 10: Δy_{panto} for the leading (a) and the trailing (b) pantograph in multiple operation at a distance of 165 m.

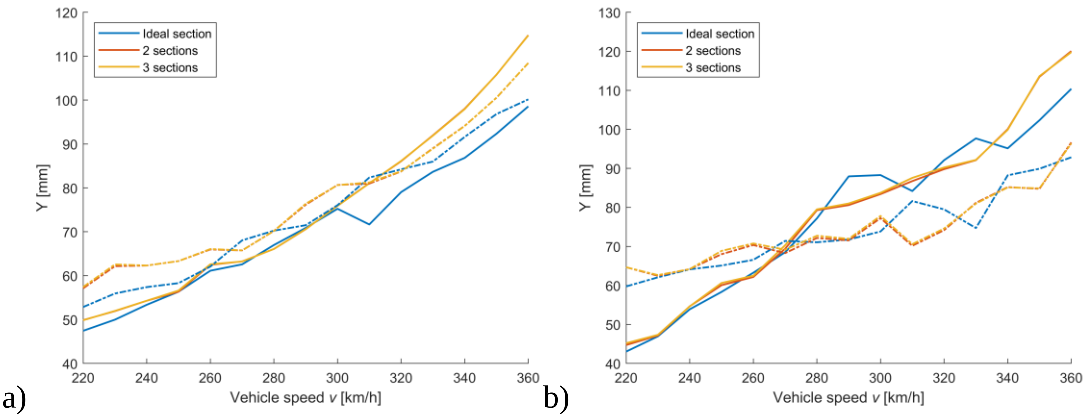

Figure 11: Δy_{StA} and Δy_{mid} (dashed) for the leading (a) and the trailing (b) pantograph in multiple operation at a distance of 165 m.

4 Conclusions and Contributions

This study shows that the results obtained from the dynamic simulations are noticeably affected by the chosen setup parameters. The most noticeable difference is obtained by changing the messenger and stitch wire's element type, initialising the pantographs in a balanced uplift position, and using free contact wire ends. The convergence study performed for the reference system AC stitched shows that reducing the element length below 0.5 m and the time step below 1 ms does not noticeably change the results in the studied frequency range up to 20 Hz. By applying the most suitable simulation settings from the convergence study, most of the required ranges of the resulting contact force dynamics set by the validation standard can be fulfilled. Exceptions are the standard deviation σ in the separate frequency ranges of 0-5 and 5-20 Hz. Especially in the 0-5 Hz range, σ consistently exceeds the required values for the trailing pantographs. The most noticeable difference is, however, the range of contact force between F_{min} and F_{max} on the trailing pantograph at 320 km/h. This shows that further investigations on the model setup relating to the methods described in the standard are recommended. This could be facilitated in a future benchmark study. The verification simulations for the new Swedish high-speed catenary system show that the system fulfils the requirements set by the TSI Energy with good margins. The comparison between the results for the ideal section and two sections with overlap shows that the latter is crucial for correctly understanding the uplift and vertical working range of the pantograph operating on the catenary. The surprisingly low difference in contact force standard deviation between the two cases should be confirmed by further investigations. Particular focus will be placed on accurately representing the catenary structure around the section overlap and modelling the operation with more than two pantographs. As these cases prove to be especially sensitive to the applied structural damping levels, further variational studies should also be performed on that aspect. There are plans to conduct field measurements on a test section of the new system in multiple operation, which will be used to calibrate the structural damping levels and confirm the overall behaviour.

Acknowledgements

The authors would like to thank Trafikverket for funding this research.

References

[1] F. Kiessling, R. Puschmann, A. Schmieder, and E. Schneider, *Contact lines for electric railways : planning, design, implementation*. Berlin: Siemens AG, 2001.

[2] J. Ambrósio, J. Pombo, M. Pereira, P. Antunes, and A. Mósca, “Recent Developments in Pantograph-Catenary Interaction Modelling and Analysis,” *Int. J. Railw. Technol.*, vol. 1, no. 1, pp. 249–278, Apr. 2012, doi: 10.4203/ijrt.1.1.12.

[3] A. Brodkorb and M. Semrau, “Simulationsmodell des Systems Oberleitungskettenwerk und Stromabnehmer,” *Elektrische Bahnen*, vol. 91, no. 4, pp. 105–113, 1993.

[4] P. Ramalho, P. Antunes, J. Ambrósio, A. M. Macedo, and S. Pissarra, "Virtual pantograph-catenary environment for control development based on a co-simulation approach," *Multibody Syst. Dyn. 2022*, pp. 1–25, May 2022, doi: 10.1007/S11044-022-09826-Z.
[5] The European Commission, "Final Report Summary - PANTOTRAIN (Pantograph and catenary interaction total regulatory acceptance for the interoperable network)," pp. 1–13, 2012.
[6] S. Bruni *et al.*, "The results of the pantograph–catenary interaction benchmark," *Veh. Syst. Dyn.*, vol. 53, no. 3, pp. 412–435, Mar. 2015, doi: 10.1080/00423114.2014.953183.
[7] European Committee for Electrotechnical Standardization, *EN 50318 – Railway applications – Current collection systems – Validation of simulation of the dynamic interaction between pantograph and overhead contact line*. 2018.
[8] T. Jiang, A. Rønnquist, Y. Song, G. T. Frøseth, and P. Nåvik, "A detailed investigation of uplift and damping of a railway catenary span in traffic using a vision-based line-tracking system," *J. Sound Vib.*, vol. 527, p. 116875, Jun. 2022, doi: 10.1016/J.JSV.2022.116875.
[9] Y. Song, T. Jiang, A. Rønnquist, P. Nåvik, and G. T. Frøseth, "The Effects of Spatially Distributed Damping on the Contact Force in Railway Pantograph-Catenary Interactions," *IEEE Trans. Instrum. Meas.*, vol. 70, 2021, doi: 10.1109/TIM.2021.3091459.
[10] *Commission Regulation (EU) No 1301/2014 of 18 November 2014 on the technical specifications for interoperability relating to the "energy" subsystem of the rail system in the Union*. The European Commission, 2014.
[11] J. Chung and G. M. Hulbert, "A Time Integration Algorithm for Structural Dynamics With Improved Numerical Dissipation: The Generalized-α Method," *J. Appl. Mech.*, vol. 60, no. 2, pp. 371–375, Jun. 1993, doi: 10.1115/1.2900803.
[12] *EN 50367. Railway applications. Fixed installations and rolling stock. Criteria to achieve technical compatibility between pantographs and overhead contact line*. European Committee for Electrotechnical Standardization, 2020.